A Reliability Assessment Approach For Integrated Transportation and Electrical Power Systems Incorporating Electric Vehicles

Kai Hou, *Student Member*, *IEEE*, Xiandong Xu, *Member*, *IEEE*, Hongjie Jia*, *Member*, *IEEE*, Xiaodan Yu, Tao Jiang, *Member*, *IEEE*, Kai Zhang and Bin Shu

***Abstract*—With the increasing utilization of electric vehicles (EVs), transportation systems and electrical power systems are becoming increasingly coupled. However, the interaction between these two kinds of systems are not well captured, especially from the perspective of transportation systems. This paper studies the reliability of integrated transportation and electrical power system (ITES). A bidirectional EV charging control strategy is first demonstrated to model the interaction between the two systems. Thereafter, a simplified transportation system model is developed, whose high efficiency makes the reliability assessment of the ITES realizable with an acceptable accuracy. Novel transportation system reliability indices are then defined from the view point of EV's driver. Based on the charging control model and the transportation simulation method, a daily periodic quasi sequential reliability assessment method is proposed for the ITES system. Case studies based on RBTS system demonstrate that bidirectional charging controls of EVs will benefit the reliability of power systems, while decrease the reliability of EVs travelling. Also, the optimal control strategy can be obtained based on the proposed method. Finally, case studies are performed based on a large scale test system to verify the practicability of the proposed method.**

***Index Terms*—Electric vehicle, electrical power system, transportation system, renewable energy, uncertainty, reliability.**

NOMENCLATURE

V_i	The i^{th} electrical vehicle
Ω_{EV}	Set of EVs
Ω_{Cnct}	Set of EVs that are connected to the grid
Ω_{Chg}	Set of EVs that are charging from the grid
$\Omega_{G2V,\max}$	The maximum G2V control set
Ω_{G2V}	G2V control set
$\Omega_{V2G,\max}$	The maximum V2G control set
Ω_{V2G}	V2G control set
ΔP_G	Power shortage
$P_{C,\mathrm{i}}$	Charging power of V_i
$P_{D,\mathrm{i}}$	Discharging power of V_i
D_{AB}	Driving distance between location A and B
δ_{Ctl}	SoC threshold for bidirectional charging control
δ_{FC}	SoC threshold for finding charging stations
δ_{CoV}	Stopping criterion of Monte Carlo simulation
ITES	Integrated transportation and electrical power system
EV	Electrical vehicles
RG	Renewable generation
G2V	Grid to vehicle
V2G	Vehicle to grid
SoC	State of charge
LOEE	Loss of energy expectation
LOLP	Loss of load probability
AFFC	Average frequency of finding charging stations
ATFC	Average extra time for charging
AFCH	Average frequency of calling for help
ATCH	Average extra time of calling for help
ATT	Average total extra time
EEG2V	Expected energy for the G2V control
EEV2G	Expected energy for the V2G control

The work was supported by Natural Science Foundation of China (51377117, 51361130152), National High-tech R&D Program of China (2015AA050403) and Royal Academy of Engineering Distinguished Fellowship of United Kingdom (DVF1415/02/59).

Kai Hou, Hongjie Jia and Xiaodan Yu are with Key Laboratory of Smart Grid of Ministry of Education, Tianjin University, Tianjin, China (hdbhyj@tju.edu.cn, hjjia@tju.edu.cn, yuxd@tju.edu.cn).

Xiandong Xu is with School of Electronics, Electrical Engineering and Computer Science, Queen's University Belfast, Belfast BT9 5AH, UK (e-mail: x.xu@qub.ac.uk).

Kai Zhang and Bin Shu are with Beijing Electric Power Economic Research Institute, Beijing, China. (13601205694@163.com, shubin0403@163. com)

Tao Jiang is with Northeast Dianli University, Jilin, China (e-mail: tjiang@nedu.edu.cn).

I. INTRODUCTION

With the rapid development of social economy, the consumption of fossil fuel grows dramatically. It brings several serious social problems, i.e. resource exhaustion, greenhouse effect, *et al*. In order to solve such problems, renewable generations (RGs) and electric vehicles (EVs) have attracted increasing attentions. These new techniques bring extra uncertainties and threats to power system reliability, while benefiting the environment on the other hand [1, 2]. The introduction of RGs will decrease the reliability of electric power systems [3, 4]. This is because their outputs strongly depend on the weather, which is uncontrollable. An effective solution is to install energy storage devices, which are able to absorb extra power at load valleys and then release it at load peaks [5]. EVs, which can be regarded as both energy storage devices and controllable loads to the grid, draw more and more concerns. They couple the transportation system and the electrical power system. When lots of EVs are applied, interactions between the two systems will be very complex and should be carefully studied.

Since EVs are charged in electrical power systems, the integration of EVs may benefits the reliability of power systems by applying charging control techniques. A detailed analysis of control modes of EVs could be found in [7-10], including modes of "grid to vehicle (G2V)" and "vehicle to grid (V2G)". In the G2V mode [7], EVs could be considered as changeable loads. They could be connected into grid to charge, or disconnected -from grid accordingly. In the V2G mode, EVs could be

considered as virtual storage devices. They could be charged with power flowing from the grid, or discharged with power sending back to the grid. An aggregation and bidirectional charging power control approach was proposed in [7] by combining the G2V and the V2G controls. This method also guaranteed that EVs could be fully charged before user's preset leaving time. A charging load self-management method was developed in [8] to mitigate the operational risk by a sequential charging control technique. A direct charging control method for EVs was provided in [9] considering consumer's comfort level. However, the above studies focused on the impact of EVs on electrical power system reliability, but few discussions took EV travelling reliability into account.

To study the reliability of the integrated transportation and electrical power system (ITES), reliability performance of both systems should be considered comprehensively [10-12]. EVs, which are coupling points of the two systems, play a significant role in the interaction chain. Thus, it is necessary to analyze the impact of EVs on power system reliability. It was indicated that the uncertain feature of EV charging loads would be adverse to power system reliability [13, 14]. However, as a type of interruptible loads, demand-side managements could be performed on EVs, and then the overall reliability of power system would be improved [15]. The impact of EVs charging on distribution system reliability was discussed considering a simple charging control technique in [16]. Reliability performance of an EV integrated system using the battery exchange mode was studied in [17]. System generation adequacy analysis were performed considering the integration of EVs in [7] and [18]. However, in order to further study the reliability of ITES, there is still a lack of quantitative reliability assessment approach incorporating both transportation and electrical power systems. Thus, it is important to establish suitable reliability indices and assessment method for the ITES system. This paper aims at providing such indices and algorithms to analyze the reliability of the ITES system.

Rest of this paper is as follows: Interaction model between the transportation system and the electrical power system is discussed in Section II. The main contributions of this paper are organized in Section III, including a simplified transportation simulation technique, a series of newly defined reliability indices, and a novel reliability assessment approach for the ITES. Numerical studies are demonstrated in Section IV and conclusions are drawn in Section V.

II. Interaction Model Between Transportation And Electrical Systems

The transportation system and the electrical system are tightly integrated by the increasing utilization of EVs. On one hand, when moving on the road, EVs transport drivers and passengers to their destinations by consuming electricity from batteries. On the other hand, when connected to the power grid, EVs absorb electricity from the grid and can be regarded as controllable loads. Therefore, it can be concluded that EVs play an essential role in the interaction between the two kinds of systems. The increasing quantity of EVs will bring in extra load demands, and may decrease the reliability of the power system. In addition, if EVs are not fully charged, they may run out of power on the road and interrupt travelling plans of drivers. Therefore, it is necessary to establish a model for EVs' charging processes to analyze the impact of the EV integration in detail.

As demonstrated in [7] and [16], the application of EV charging control techniques will benefit the reliability of the electrical system. This is basically because EVs with charging controls can be regarded as auxiliary power storages to bridge the gap between power generation and load consumption. Therefore, a bidirectional charging control strategy is introduced into this paper to model the interaction between the two systems. As indicated in [7], such control strategy contains two basic modes, which are the grid to vehicle mode (G2V) and the vehicle to grid mode (V2G). Detailed models of those two modes are demonstrated as follows.

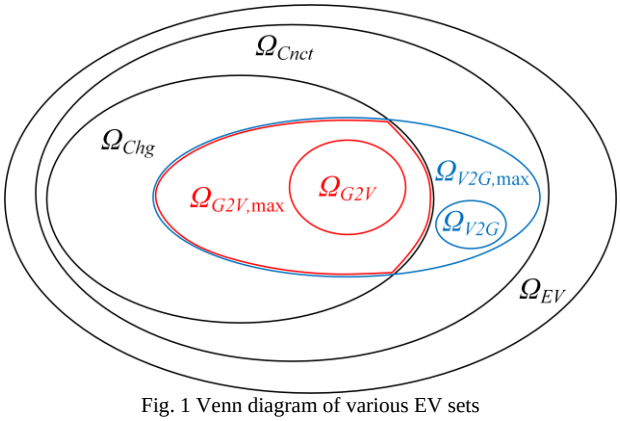

Fig. 1 Venn diagram of various EV sets

Denote the total number of EVs as N_{EV}, then the EV set of the transportation system can be represented by $\Omega_{EV}=\{V_1, V_2, \dots, V_{N_{EV}}\}$, where V_i refers to the ith EV. In order to quantify charging states of EVs, we assign each EV a parameter called state of charge (SoC), which is defined as

$$SoC_i = \frac{E_i}{E_{N,i}} \tag{1}$$

where $E_{N,i}$ and E_i are rated and remaining battery capacity of V_i, respectively.

It can be seen that EVs in Ω_{EV} can be divided into two groups. One group involves those on the road, while the other one contains all EVs that are connected to the grid. Define the second group as $\Omega_{Cnct}=\{V_1, V_2, \dots, V_{n_{Cnct}}\}$, where n_{Cnct} is the number of connected EVs. It can also be notice that some EVs in Ω_{Cnct} have already been fully charged, and can no longer absorb power from the grid. Therefore, the charging EVs can be denoted by Ω_{Chg}, as follows:

$$\Omega_{Chg} = \{V_i \mid SoC_i < 100\%, V_i \in \Omega_{Cnct}\} \tag{2}$$

In order to visually display the relationship among the defined EV sets, a Venn diagram is drawn in Fig. 1.

A. G2V Control Model

The basic idea of the G2V control is to disconnect several charging EVs from the grid, such that power supply shortage can be alleviated. Thus, the key problem is to decide which charging EVs should be disconnected. Generally, in order to satisfy travelling demands of drivers, the G2V control should not be performed on EVs with unduly low SoC. Therefore, a threshold δ_{Ctl} is utilized to obtain a maximum G2V control set $\Omega_{G2V,\max}$, as shown in Fig. 1. It can be achieved by

$$\Omega_{G2V,\max} = \{V_i \mid SoC_i > \delta_{Ctl}, V_i \in \Omega_{Chg}\} \tag{3}$$

When load demand exceeds power supply, EVs in $\Omega_{G2V,\max}$ can be disconnected from the grid to alleviate the power shortage. The maximum G2V control power $P_{G2V,\max}$ can be obtained when all EVs in $\Omega_{G2V,\max}$ are disconnected, as follow:

$$P_{G2V,\max} = \sum_{V_i \in \Omega_{G2V,\max}} P_{C,i} \tag{4}$$

where $P_{C,i}$ is the charging power of V_i.

Denote the power shortage as ΔP_G, which can be obtained by

$$\Delta P_G = \max\left(P_{G,Total} - P_{L,\text{Total}} - \sum_{V_i \in \Omega_{Chg}} P_{C,i} - P_{Loss}, 0 \right) \tag{5}$$

where $P_{G,Total}$ is the power generation capacity, $P_{L,Total}$ is the total electric load without EVs, $\sum_{V_i \in \Omega_{Chg}} P_{C,i}$ is the total charging power of EVs and P_{Loss} is the network loss.

Then $\Delta P_G>0$ indicates that power consumers are lack of electrical supply. Under this circumstance, the G2V control should be performed. It can be seen that if $0<\Delta P_G \leqslant P_{G2V,\max}$, the power shortage can be completely eliminated by the G2V control. Generally, EVs with higher *SoC* have priories over those with lower *SoC*. Therefore, EVs in $\Omega_{G2V,\max}$ should be sorted in descending order by their *SoC* values. Then the G2V control set Ω_{G2V} can be obtained by

$$\Omega_{G2V} = \left\{ V_j \mid j \le n_{G2V}, V_j \in \Omega_{G2V,\max} \right\} \tag{6}$$

where n_{G2V} is the number of EVs with the G2V control, which can be calculated by

$$\min \quad n_{G2V} \tag{7}$$

$$s.t. \quad \sum_{j=1}^{n_{G2V}} P_{C,j} \ge \Delta P_G, V_j \in \Omega_{G2V,\max} \tag{8}$$

$$\sum_{j=1}^{n_{G2V}-1} P_{C,j} < \Delta P_G, V_j \in \Omega_{G2V,\max} \tag{9}$$

Then the power shortage can be relieved by disconnecting all charging EVs in Ω_{G2V}.

B. V2G Control Model

When the power shortage is too large for the G2V control to eliminate, the V2G control can be used as a complement. The V2G control not only suspends some EVs from charging, but also makes them discharge power back to the grid. Thus, the V2G control mode has more potential than the other one. Different from the G2V control, the V2G control could be performed on any connected EVs. So the maximum V2G control set $\Omega_{V2G,\max}$ can be obtained by

$$\Omega_{V2G,\max} = \left\{ V_i \mid SoC_i > \delta_{Ctl}, V_i \in \Omega_{Cnct} \right\} \tag{10}$$

Then the maximum V2G control power $P_{V2G,\max}$ is

$$P_{V2G,\max} = \sum_{V_i \in \Omega_{V2G,\max}} P_{D,i} \tag{11}$$

where $P_{D,i}$ is the discharging power of V_i.

When $P_{G2V,\max}<\Delta P_G<P_{V2G,\max}+P_{G2V,\max}$, the G2V control is not able to relieve the power shortage. Therefore, the V2G control should also be performed. Similar to the G2V mode, EVs in $\Omega_{V2G,\max}$ should also be sorted in descending order by their *SoC*. Then the V2G control set Ω_{V2G} can be obtained by

$$\Omega_{V2G} = \left\{ V_j \mid j \le n_{V2G}, V_j \in \Omega_{V2G,\max} \right\} \tag{12}$$

where n_{V2G} is the number of EVs with the V2G control, which can be calculated by

$$\min \quad n_{V2G} \tag{13}$$

$$s.t. \quad \sum_{j=1}^{n_{V2G}} P_{D,j} \ge \Delta P_G - P_{G2V,\max}, V_j \in \Omega_{G2V,\max} \tag{14}$$

$$\sum_{j=1}^{n_{V2G}-1} P_{D,j} < \Delta P_G - P_{G2V,\max}, V_j \in \Omega_{G2V,\max} \tag{15}$$

Then the power shortage can be relieved by disconnecting all EVs in $\Omega_{G2V,\max}$, and making EVs in Ω_{V2G} discharge power back to the grid.

It is noticeable that when $\Delta P_G>P_{V2G,\max}+P_{G2V,\max}$, both G2V and V2G controls are not able to eliminate the power shortage. Under this situation, load curtailment is inevitable to balance power demand and supply. Denote it as P_{LC}, then it can be obtained by the DC optimal power flow provided by the Matpower toolbox. Parallel computing technique can be used to enhance the calculation efficiency.

In reality, EV drivers will respond the charging control of power grid only if the compensation is attractive. Therefore, the power grid has to make a compensatory price for EV drivers who participate in the charging control. Even so, some EV drivers may still decide not to respond the charging control. Therefore, a participation probability parameter p_{pert} to simulate their decisions is introduced in this paper.

III. A Reliability Assessment Method for the ITES System

The increasing EV penetration will bring extra load demands to the power system, and may severely affect its reliability. As demonstrated in the last section, the power shortage can be relieved by applying the bidirectional charging control strategy. However, such technique is adverse to the charging efficiency of EVs, and may decrease their travelling distances. In general, G2V and V2G techniques will benefit the reliability of the electrical system, while reducing the reliability of the transportation system. Therefore, it is necessary to establish a new approach to assess the reliability of the integrated transportation and electrical system, incorporating the interaction between the two systems. In this section, a simplified transportation simulation algorithm is first developed to speed up the transportation system simulation. Then a daily periodic quasi sequential Monte Carlo simulation based reliability assessment approach is proposed for the ITES system.

A. Transportation System Simulation Method

Traditionally, travelling schedule models [19] and optimum route algorithms can be used to simulate travelling behaviors of EVs. However, such techniques are unduly inefficient for reliability assessment, which generally has to simulate the target system for hundreds of sampled years. Therefore, the essential problem is to improve the efficiency of the transportation system simulation method to an acceptable level for reliability assessment. Inspired by [19], [20] and [10], a simplified travelling simulation method is proposed here based on a rectangular coordinate roads model to speed up the simulation. With this approximated model, optimum route algorithms, which are considerably time consuming, are no longer necessary.

1) Sampling of EV Daily Travelling Schedule

Typically, EVs are connected to the power grid only when they are at home, work units or charging stations. Thus, in order to obtain the time and duration of EVs connection, their daily travelling schedule should be determined. Similar to the internal combustion engine vehicle (ICEV), the primary mission of EVs is to fulfill drivers' transportation requirements. An activity based travelling schedule model was proposed in [19], which is

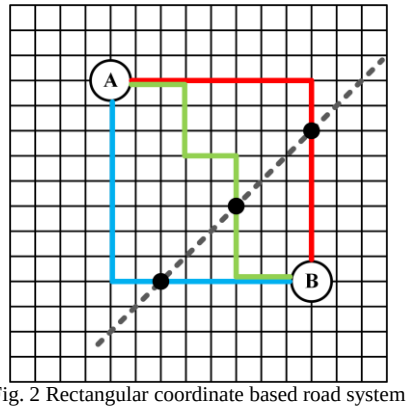

Fig. 2 Rectangular coordinate based road system

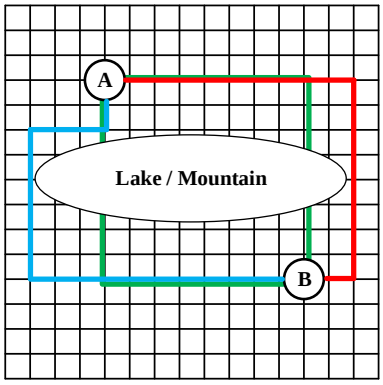

Fig. 3 There is a lake / mountain in the target city.

simplified and used in this paper. Assuming that travelling destinations of EVs include hospitals, work units, shopping malls, scenic spots, et al. Then EVs will travel among such places and return home at the end of a day. Therefore, it is reasonable to simulate EV travelling schedules day by day. Daily visiting frequencies of those locations can be obtained based on statistical data

$$f_\alpha = \frac{n_\alpha}{n_{day}} \tag{16}$$

where $\alpha \in$ {hospitals, work units, shopping malls, scenic spots}; f_α is the daily frequency that α will be visited; n_α is total visiting times of α and n_{day} is the number of statistical days.

After obtaining f_α, EV daily travelling schedule can be sampled. After that, sampled destinations should be sorted. In our daily life, work units are usually the first destinations after leaving home. Therefore, work unit is fixed in the first place of EV daily travelling plan, and other sampled destinations are randomly permutated.

2) Distance Calculation

The driving distance between adjacent destinations should be calculated to determine EV's battery consumption. Traditionally, optimum route algorithms can be applied to path selection problems. However, for reliability assessment based issues, decades or even hundreds of sampling years will be simulated. Due to the large quantity of EVs, the inefficiency of optimum route algorithms and the long simulation time scale, the computation efficiency of such a complex problem becomes unacceptable. A straightforward idea is to replace the inefficient optimum route algorithm by a simple one. Inspired by [20], which simplified transportation systems into two- dimensional meshes, a hypothesis is introduced that roads in transportation network are either paralleled or vertical to each other. Then traffic system can be easily integrated into rectangular coordinates, as shown in Fig. 2.

It can been seen that there are several optional paths between location A and B, i.e. red, green and blue lines in the figure. However, due to the features of the rectangular coordinate, they have the same distance. Therefore, driving distance D_{AB} between A and B can be easily obtained with their coordinates:

$$D_{AB} = \left|x_A - x_B\right| + \left|y_A - y_B\right| \tag{17}$$

where x and y are the horizontal and vertical coordinates.

Notice that there may be lakes or mountains in the target city, so the distance calculation process has to be modified in this circumstance. As shown in Fig. 3, if the lake / mountain is larger than the green rectangle determined by location A and B, driving distance D_{AB} can no longer be obtained using (17).

Define the minimum and maximum horizontal coordinate of the lake / mountain as x_1 and x_2, respectively, then D_{AB} can be obtained by

$$D_{AB} = \left|x_A - x_B\right| + \left|y_A - y_B\right| + 2\min\left\{\left|x_A - x_1\right|, \left|x_B - x_2\right|\right\} \tag{18}$$

If the lake / mountain is larger than the rectangle in the vertical axis, then x_1 and x_2 in (18) should be changed to the minimum and maximum vertical coordinate y_1 and y_2, respectively.

In the real world, roads may not be orthogonal. In addition, drivers may not go the shortest path. Therefore, the normal distribution is used in origin destination analysis to solve this problem [10]. The idea is introduced in this paper as follows:

$$D_{EV} \sim N\left(D_{AB}, \left(kD_{AB}\right)^2\right) \tag{19}$$

where D_{EV} is the actual driving distance of EV; k is a preset standard deviation parameter of D_{AB}.

3) Location Sampling

When the *SoC* of EVs is lower than a preset threshold δ_{FC}, drivers will suspend their current travelling plan and head to the nearest charging station immediately. Under this situation, EV daily travelling schedules should be modified. Before further analysis, it is necessary to determine the current location of the low power EV. With the rectangular coordinate roads assumption, there are multiple shortest paths between the starting point and the destination. However, no matter which path does the driver select, the low battery location of the EV will always be on a line with a slope 1.0, i.e. the gray dotted line in Fig. 2. It can be seen that driving distances from the start point A to any points on the gray line are exactly the same. This feature enable us to sample locations of EVs at any given time. The equation of this line is as follows:

$$\begin{cases} y = k\left(x - x_0\right) + y_0 \\ \min\left(x_A, x_B\right) < x < \max\left(x_A, x_B\right) \\ \min\left(y_A, y_B\right) < y < \max\left(y_A, y_B\right) \end{cases} \tag{20}$$

where k, x_0 and y_0 are determined by

$$k = -\mathrm{sgn}\left(\frac{y_B - y_A}{x_B - x_A}\right) \tag{21}$$

$$x_0 = x_A + \left(x_B - x_A\right)D\% \tag{22}$$

$$y_0 = y_A + \left(y_B - y_A\right)D\% \tag{23}$$

$$D\% = \frac{D_{current}}{D_{AB}} \tag{24}$$

where sgn is the sign function and $D_{current}$ is current driving

distance between A and B.

When the above line is obtained, the current location of EV can be sampled from all intersections of the line and road network. Thereafter, distances from the current location to any charging stations can be easily obtained by (17), and the nearest charging station can be chosen accordingly. Then the daily travelling schedule can be updated by adding the selected charging station into the original EV travelling plan.

Another unavoidable situation is that EVs may break down on road if their batteries run out. Under this circumstance, drivers have to call for help, then additional time costs are inevitable. The EV daily travelling schedule can also be updated with the proposed method.

B. Reliability Assessment of ITES System

With the proposed transportation system simulation method, EV behaviors can be analyzed efficiently. Then reliability assessment of the ITES system can be performed accordingly. However, there is still a lack of quantified reliability indicators for the EV integrated transportation system. Therefore, based on load demands of electricity consumers and travelling requirements of EV drivers, a series of reliability indices are established for the ITES system. Thereafter, a reliability assessment approach is proposed to calculated such indices

1) Reliability Indices of ITES System

Quantified indices are the foundation of reliability assessment. For the power system, traditional generation adequacy indices can be used to quantify its reliability [21]:

Loss of Energy Expectation (LOEE, MWh/year) is the expected loss of energy caused by load curtailments

$$LOEE = \frac{\int_0^{T_{MCS}} P_{LC,t}\,dt}{T_{MCS}} \tag{25}$$

where T_{MCS} is the simulation time scale of the MCS, measured by year; $P_{LC,t}$ is the load curtailment at time t.

Loss of Load Probability (LOLP) refers to the probability of load curtailments

$$LOLP = \frac{\int_0^{T_{MCS}} u\left(P_{LC,t}\right)dt}{T_{MCS}} \tag{26}$$

where $u(P_{LC,t})=1$, if $P_{LC,t}\neq 0$; and $u(P_{LC,t})=0$, otherwise.

For EV integrated transportation systems, new reliability indices are developed. For circumstances that EVs have to find charging stations for battery charging, extra time is requested on additional driving distance and battery charging. Suppose an EV runs out of power at location C on its way to location D. If the nearest charging station is at location F. Then additional travelling distance ΔD can be calculated by

$$\Delta D = D_{CF} + D_{FD} - D_{CD} \tag{27}$$

Two indices are introduced to quantify the impact of this kind of situations on the EV travelling reliability, as follows:

Average frequency of finding charging stations (AFFC, times/year) is the average frequency for an EV to find charging stations in a year

$$AFFC = \frac{\sum_{i=1}^{N_{EV}} N_{i,FC}}{N_{EV}T_{MCS}} \tag{28}$$

where $N_{i,FC}$ is the total times for V_i to find charging stations.

Average extra time for charging (ATFC, h/year) is the average extra time cost for an EV to find charging stations in a year

$$ATFC = \frac{\sum_{i=1}^{N_{EV}}\sum_{j=1}^{N_{i,FC}}\left(\Delta D_{i,j,FC}/v_i + T_{i,j,C}\right)}{N_{EV}T_{MCS}} \tag{29}$$

where $\Delta D_{i,j,FC}$ and $T_{i,j,C}$ are the additional travelling distance and the charging duration for V_i, when it goes to find charging stations for the jth time; v_i is the travelling speed of V_i.

When EVs run out of power, drivers have to call for help, costing plenty of extra time. Two indices are developed for this type of emergencies, as follows:

Average frequency of calling for help (AFCH, times/year) refers to the average frequency for an EV to call for help in a year

$$AFCH = \frac{\sum_{i=1}^{N_{EV}} N_{i,CH}}{N_{EV}T_{MCS}} \tag{30}$$

where $N_{i,CH}$ is the total times for V_i to call for help.

Average extra time for calling for help (ATCH, h/year) is defined as the average extra time cost for an EV to call for help in a year

$$ATCH = \frac{\sum_{i=1}^{N_{EV}}\sum_{j=1}^{N_{i,CH}}\left(T_{i,j,W} + T_{i,j,C}\right)}{N_{EV}T_{MCS}} \tag{31}$$

where $T_{i,j,W}$ and $T_{i,j,C}$ are the waiting and charging duration for V_i, when it calls for help for the jth time.

By adding up ATFC and ATCH, average total extra time (ATT) can be obtained, as follow:

$$\mathrm{ATT} = \mathrm{ATFC} + \mathrm{ATCH} \tag{32}$$

Two more indices are developed to quantify how much battery capacity is participated in G2V and V2G controls:

Expected energy for the G2V control (EEG2V, MWh/year) is the expected energy that participates in the G2V control

$$EEG2V = \frac{\int_0^{T_{MCS}} \sum_{V_i\in\Omega_{k,G2V}} P_{C,i,t}\,dt}{T_{MCS}} \tag{33}$$

where $\Omega_{k,G2V}$ is the G2V control set at time t.

Expected energy for the V2G control (EEV2G, MWh/year) is the expected energy that participates in the V2G control

$$EEV2G = \frac{\int_0^{T_{MCS}} \sum_{V_i\in\Omega_{k,V2G}} P_{D,i,t}\,dt}{T_{MCS}} \tag{34}$$

where $\Omega_{k,V2G}$ is the V2G control set at time t.

2) Daily Periodic Quasi Sequential Monte Carlo Simulation Based Reliability Assessment Approach for the ITES System

In order to provide the reliability indices defined above, appropriate assessment method has to be developed to accommodate probabilistic characteristics of the ITES system. Generally, operating/failure process of generating unit can be modeled by the two state Markov chain model. Because of their "memoryless" feature, such model can be simulated by either sequential or nonsequential Monte Carlo techniques. However, only the sequential one can be applied to the ITES system, because EV travelling behaviors are correlated in time domain. For the traditional sequential Monte Carlo simulation method, operation processes of generating units and travelling behaviors of EVs should all be sampled and stored to calculate the indices. Considering the large quantity of EVs and the long simulation years, such method need a huge memory space to store all those sampled data. Therefore, it has to be modified to adapt to the

This article has been accepted for publication in a future issue of this journal, but has not been fully edited. Content may change prior to final publication. Citation information: DOI 10.1109/TSG.2016.2545113, IEEE Transactions on Smart Grid

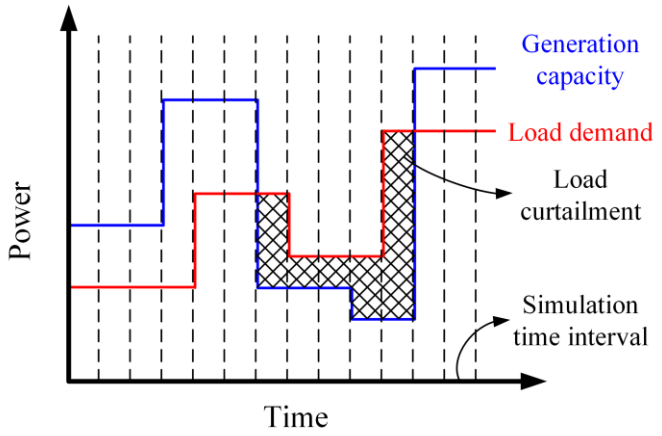

Fig. 4 The quasi sequential Monte Carlo simulation technique

ITES system.

For the transportation system, it can be notice that all EVs begin their journeys at the morning, and return home after travelling for a whole day. Then it can be concluded that EV travelling schedules in different days are independent from each other. Therefore, EV travelling behaviors can be periodically sampled by each day, then memory space requirements will be considerably reduced.

For the electrical system, a time discretization technique detailed in Appendix can be utilized [22]. With this technique, quasi sequential Monte Carlo simulation [23] can be performed and the assessment process is further simplified, as shown in Fig. 4. Such technique is applied to this paper and all integral operations in (25)-(34) are simplified into summation operations.

With this technique, operation/failure processes of generation units can be sampled by calculating the state transit probability $P_{u,ST}$ for each generation unit, as follow:

$$p_{u,ST} = 1 - e^{\lambda_u \Delta t} \approx \lambda_u \Delta t \tag{35}$$

where Δt is the time interval. u refers to the uth generation unit. When u is operating, λ_u is the outage rate, otherwise, λ_u is the repair rate.

Generate a random number $R_u \in [0, 1]$. Then operation state $s_{u,t}$ of u at time t is determined by

$$s_{u,t} = \begin{cases} s_{u,t-\Delta t}, & R_u \geq p_{u,ST} \\ 1 - s_{u,t-\Delta t}, & R_u < p_{u,ST} \end{cases} \tag{36}$$

Thus, the total generation capacity at time t is

$$P_{G,Total,t} = \sum_{u=1}^{N_G} P_{G,u} s_{u,t} \tag{37}$$

The power shortage ΔP_G can then be calculated by (5), and the charging control can be performed accordingly.

In order to provide effective reliability indices, appropriate load models are also necessary. Generally, time varying loads and annual hourly load curves [21] are two commonly used load models for reliability assessment. The first one is more comprehensive and allows different load curves for each bus. On the contrary, the latter one models the system as a whole. In this paper, an annual load curve [25] is used to model the electricity demand of the ITES system.

By combining this method with the bidirectional charging control technique (Section II) and the transportation system simulation method (Section III A), a daily periodic quasi sequential Monte Carlo simulation based approach is developed

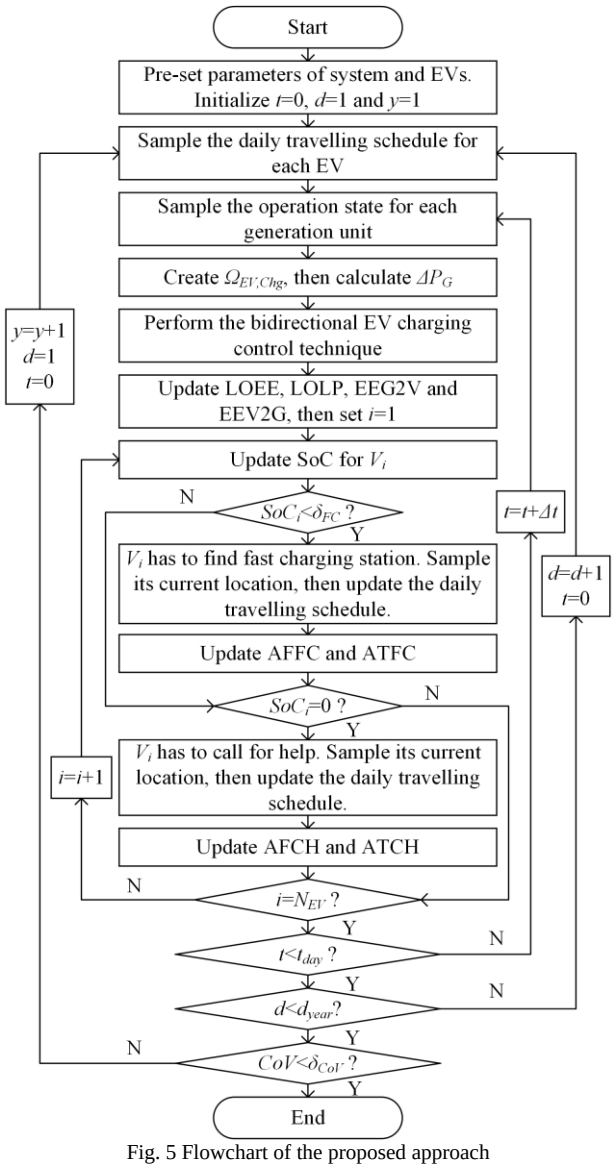

Fig. 5 Flowchart of the proposed approach

to assess the reliability of the ITES system. The overall procedure of the proposed approach is as follows:

Step 1: Initialize power system parameters, i.e., outage rate λ, repair rate μ and load curve $L(t)$, *et al*. Initialize EVs parameters, i.e. rated battery capacity E_r, rated charging and discharging power P_C and P_D, *et al*. Initialize simulation time interval Δt, convergence criterion δ_{CoV}. Initialize simulation timers.

Step 2: Create the daily travelling schedule for each EV.

Step 3: Update the operating state for each generation unit by (35)-(36), then calculate the total generation capacity by (37)

Step 4: Create Ω_{Chg} by (2). Then determined ΔP_G by (5).

Step 5: If ΔP_G>0, which means generation shortage occurs, use the bidirectional charging control (Section II) to balance the generation and load. Then create Ω_{G2V} and Ω_{V2G}, and update charging or discharging states of EVs accordingly.

Step 6: Calculate P_{LC} by DC OPF algorithm. Update LOEE, LOLP, EEG2V and EEV2G by (25), (26), (33) and (34), respectively. Then set EV counter i=1.

Step 7: Update the SoC_i of V_i.

Step 8: If SoC_i is lower than δ_{FS}, V_i suspends its current travelling plan and goes to the nearest charging station for battery charging. Its daily travelling schedule is modified

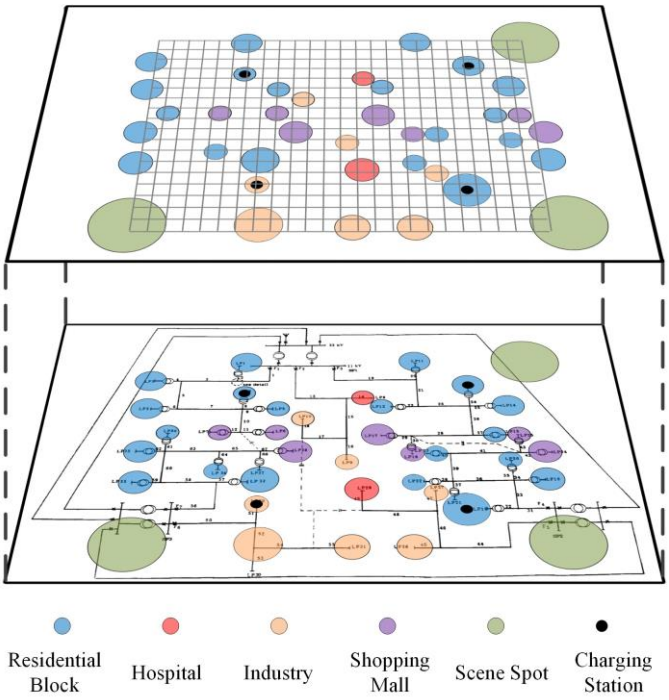

Fig. 6 Basic structure of the RBTS base test system

accordingly. Then update AFFC and ATFC by (28) and (29).

Step 9: If SoC_i=0, V_i runs out of power. Then V_i has to terminate its travelling and calls for help. Its daily travelling schedule is modified accordingly. Then update AFCH and ATCH by (30) and (31), respectively.

Step 10: If $i<N_{EV}$, set $i=i+1$ and loop to Step 7. Otherwise, go to Step 11.

Step 11: Denote the terminal time of a day as t_{day}. If $t<t_{day}$, set $t=t+\Delta t$ and loop back to Step 3. Otherwise, go to Step 12.

Step 12: Denote the terminal day of a year as d_{year}. If $d<d_{year}$, set $d=d+1$, $t=0$ and loop to Step 2. Otherwise, go to Step 13.

Step 13: If the stoping criterion is not satisfied, set $y=y+1$, $d=1$, $t=0$ and loop to Step2. Otherwise, save and output results.

IV. Numerical Results

Case studies are performed on a RBTS [24] based ITES system to examine the performance of the proposed approach. Impacts of RG and EV penetrations are analyzed in details. Then, the practicability of this method is verified in a large scale test case, which is established based on the Beijing central transportation system and the RTS system [25]. The studies are performed on a PC with Intel Core i3 Quad CPU 3.40 GHz and 2.00 GB RAM.

A. A RBTS Based Test Case

The RBTS system [24] is a composite power system with 6 buses, 11 generator units, 9 branches, 2 generation (PV) buses and 4 load (PQ) buses. The total generation capacity is 240 MW. Its peak load is 185 MW and an annual load curve is used [25]. Wind power generators are introduced at bus 2. Variations of wind speed can be represented by Weibull distributions, whose parameters are obtained based on the historical data from [26]. Ref. [27] illustrates the distribution system of bus 4 in detail, as dipicted in the lower layer of Fig. 6. There are 38 load points and three customer types in this system, including residential, small user and commercial. This system is regarded as a small city so as to test the performance of the proposed approach. Locations of residential blocks, hospitals, industries, malls and scene spots are assigned based on the customer type of load points. A perpendicular road system is attached to the distribution system, as shown in the upper layer of Fig. 6. Distance between adjacent roads is 1 km. In additional, four charging stations are introduced into this system. In order to cover as large area as possible, they are placed in the four directions of the system (load point 4, 13, 18 and 29). The ITES system is presented in Fig. 6 in detail.

Table I Parameters of the RBTS based test case

Parameter	Value
PV penetration	30%
EV penetration	10%
SoC threshold for bidirectional charging control (δ_{Ctl})	60%
SoC threshold for finding charging station (δ_{FC})	20%
Convergence criterion of MCS (δ_{CoV})	0.01
Simulation time interval of MCS (Δt, hour)	1/6
EV rated capacity (E_r, kWh)	U(5,20)
EV rated charging power (P_C, kW)	U_d(3,5)
EV travelling speed (v, km/h)	N(21,10)
EV charging and discharging efficiency (η)	0.95
participation probability parameter (p_{pert})	0.95

Table II Assessment results of the RBTS test case

LOEE (MWh/y)	LOLP	AFFC (times/y)	ATFC (h/y)
1022	0.0095	1.0526	1.0824
AFCH (times/y)	**ATCH (h/y)**	**ATT (h/y)**	**CPU Time (10^5s)**
0.4623	1.0025	2.0849	1.925

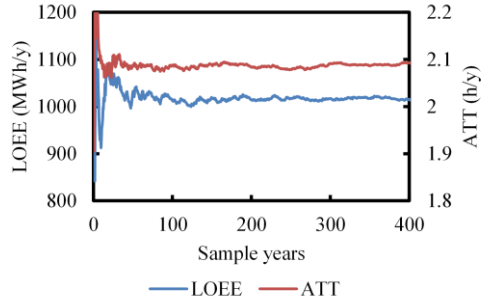

Fig. 7 Convergence curves of reliability indices

Table III Assessment results under various δ_{Ctl}

δ_{Ctl}	LOEE (MWh/y)	ATT (h/y)	EEG2V (MWh/y)	EEV2G (MWh/y)
100%	2057	1.6367	0	0
80%	1289	1.8972	676	727
60%	1022	2.0849	1001	951
40%	986	2.6544	1040	1037
20%	970	6.5917	1086	1055
0%	952	12.4112	1186	1082

It can be found in [28] that the ratio between vehicle number and electric loads in England is about 835. Therefore, we assume that there are 33411 vehicles in this system. Some other parameters are shown in Table I.

The proposed approach is used to assess the reliability of this system. Results are shown in Table II. Among all those indices, LOEE and LOLP are used to quantify the reliability of power system. AFFC, ATFC, AFCH and ATCH are transportation system reliability indices. The MCS has to sample the operation states of the ITES for 400 years to reach its stopping criterion. (δ_{CoV}<0.01), as shown in Fig. 7. The total CPU time consumption is 1.925 ×10^5 seconds.

1) Impact of SoC threshold

This article has been accepted for publication in a future issue of this journal, but has not been fully edited. Content may change prior to final publication. Citation information: DOI 10.1109/TSG.2016.2545113, IEEE Transactions on Smart Grid

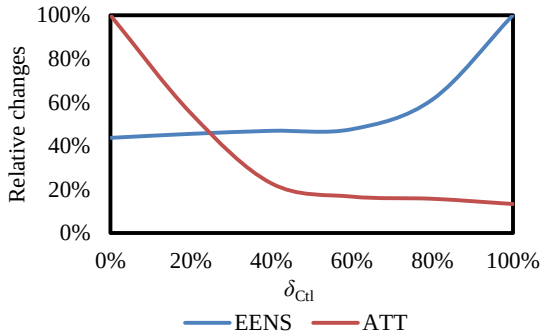

Fig. 8 Variation curve of LOEE and ATT

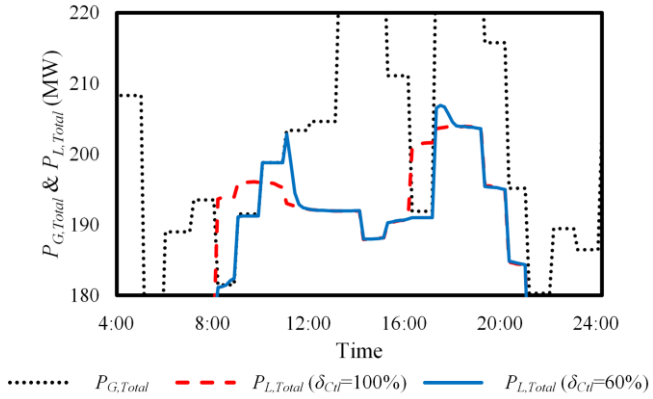

Fig. 9 Daily generation can load curves with various δ_{Ctl}

The proposed approach can be used to analyze the interaction between the two systems in detail. In order to study the impact of *SoC* threshold, a series of test cases are performed by altering δ_{Ctl}. LOEE and ATT are used to quantify reliabilities of the two systems, respectively. EEG2V and EEV2G are also calculated, as presented in Table III.

It can be seen from Table III that with the decrease of δ_{Ctl}, LOEE decreases, while ATT, EEG2V and EEV2G increase. It is because a higher δ_{Ctl} leads to larger $\Omega_{G2V,\max}$ and $\Omega_{V2G,\max}$. Then more EVs can participate in the bidirectional charging control, and sacrifice their battery capacities to support power system. Therefore, reliabilities of both systems can be affected by δ_{Ctl}.

Relative changes of LOEE and ATT are further studied to determine the optimal value of δ_{Ctl}, as shown in Fig. 8. These indices are normalized based on their maximum values. For LOEE, the maximum value can be obtained when δ_{Ctl}=100% (which means EV charging controls are not performed). For ATT, base values are obtained when δ_{Ctl}=0%.

It can be seen that the LOEE curve is generally an ascending function of δ_{Ctl}, while the ATT curve is a descending one. It can be found that δ_{Ctl} has almost no impact on LOEE when it drops below 60%. Whereas, when δ_{Ctl}<40%, ATT decreases dramatically. In general, when δ_{Ctl} ranges from 40% to 60%, both LOEE and ATT stay at a relatively low level. Therefore, the optimal δ_{Ctl} is set to 60% in this paper to enhance the reliability of the electrical power system, while maintaining the reliability of the transportation system.

Further studies are conducted to analyze the impact of δ_{Ctl} on the daily load curve. A typical day is selected from the whole year, and daily generation and load curves with various δ_{Ctl} are drown in Fig. 9.

As shown in Fig. 9, when δ_{Ctl}=100%, load demand will exceed generation capacity at 8:00 and 16:00. However, when δ_{Ctl}=60%, peak loads are partially shift to the off-peak time, and load curtailments are no longer happened. This fact demonstrates that with proper charging controls, EVs can be regarded as auxiliary energy storages for load shifting.

Table IV Impact of EV penetration on reliability indices (δ_{Ctl}=100%)

EV Pntt	LOEE (MWh/y)	ATT (h/y)	EEG2V (MWh/y)	EEV2G (MWh/y)
0%	1975	0.0000	0	0
10%	2057	1.6367	0	0
20%	2484	1.7282	0	0
30%	2970	1.7878	0	0

Table V Impact of EV penetration on reliability indices (δ_{Ctl}=60%)

EV Pntt	LOEE (MWh/y)	ATT (h/y)	EEG2V (MWh/y)	EEV2G (MWh/y)
0%	1975	0.0000	0	0
10%	1022	2.0849	1001	951
20%	783	2.2574	2840	1504
30%	1041	2.8854	5567	1795

Table VI Impact of RG penetration on reliability indices (δ_{Ctl}=100%)

RG Pntt	LOEE (MWh/y)	ATT (h/y)	EEG2V (MWh/y)	EEV2G (MWh/y)
0%	22	1.8724	0	0
10%	587	1.7952	0	0
20%	1149	1.6099	0	0
30%	2057	1.6367	0	0
40%	10921	1.7420	0	0

Table VII Impact of RG penetration on reliability indices (δ_{Ctl}=60%)

RG Pntt	LOEE (MWh/y)	ATT (h/y)	EEG2V (MWh/y)	EEV2G (MWh/y)
0%	22	1.9177	0	0
10%	211	1.7802	149	221
20%	656	1.7995	588	599
30%	1022	2.0849	1001	951
40%	6320	5.2170	5879	7112

2) Impact of EV Penetration

With the increasing EV penetration, additional uncertain load will be brought into power system. However, more EVs battery capacity can be utilized to perform load shifting. Therefore, the impact of EV penetration is further analyzed. Case studies are performed with different δ_{Ctl}, as shown in Table IV and V.

It can be seen from Table IV that when δ_{Ctl}=100%, LOEE increases along with EV penetration growing. This is because the charging control strategy cannot be performed under this situation, and the increasing EV number brings extra load to the power system. However, when δ_{Ctl}=60%, reliability of power system is improved due to the G2V and V2G control techniques, as shown in Table V. In addition, it can be noticed that LOEE is minimized when EV penetration is 20%. It is because when there are too many charging EVs, the total charging load will be too high to be shifted by charging control techniques. By comparing the above two tables, it can be found that the implementation of EV charging controls bring only a little extra reliability decline to the transportation system. Therefore, for the given power network, 20% of EV penetration can be well supported. For a larger EV penetration, additional generation capacity is indispensable.

It can also be noticed that when PV penetration is above 20%, EEG2V is lower than EEV2G. This is because G2V control has a higher priority.

3) Impact of RG Penetration

With the increasing RG penetration, extra uncertainty will be brought in power generations, resulting in lower system reliability. Therefore, the impact of RG penetration is further analyzed, as shown in Table VI and VII.

It is obvious that LOEE grows rapidly along with the

This article has been accepted for publication in a future issue of this journal, but has not been fully edited. Content may change prior to final publication. Citation information: DOI 10.1109/TSG.2016.2545113, IEEE Transactions on Smart Grid

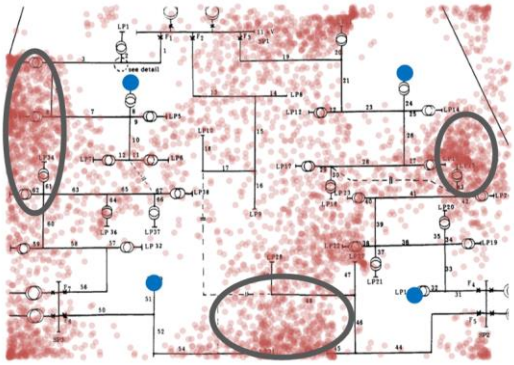

(a) Original Case

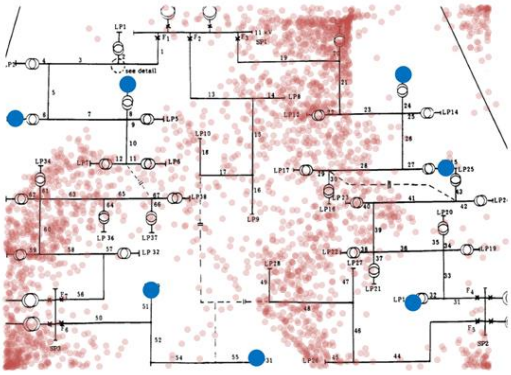

(b) Planned Case

Fig. 10 Location that EVs run out of power

Table VIII Assessment results of the RBTS test case

LOEE (MWh/y)	LOLP (times/y)	AFFC (times/y)	ATFC (h/y)
1004	0.0091	0.0104	1.3145
AFCH (times/y)	ATCH (h/y)	ATT (h/y)	CPU Time (10^5s)
0.1895	0.2987	1.6132	1.870

increase of RG penetration, while ATT remains stable. However, by comparing these two tables, it can be concluded that LOEE will be halved when EV charging controls are performed. In addition, its impact on the transportation system reliability is relatively low when RG penetration is lower than 30%. This study verified that EVs can be regarded as energy storages to balance RG variations. Another notable phenomenon is that when RG penetration is above 40%, both LOEE and ATT increase dramatically. Thus, for the given system, RG penetration should be limited below 40%.

4) Reliability Based Charging Station Planning

With the increasing penetration of EVs, additional charging stations are needed to maintain the reliability of EVs. An intuitive idea is to construct new charging stations at the place where EVs are most likely to exhaust their power. Such idea can be performed with the proposed reliability assessment approach. When performing this approach, travelling behaviors of all EVs are simulated to calculate transportation system reliability indices. Therefore, locations that EVs run out of power can be conveniently recorded for further analysis. For the case shown in Table II, such locations can be found in Fig. 10(a).

It can be seen that there is almost no red point around the four blue points, indicating that battery exhaustions rarely happen near charging stations. However, for the places that are far away from those blue points, red points are densely distributed, which means numerous EVs run out of power at those places. Therefore, it is reasonable to construct new charging station at the locations with the densest red points, as shown in the figure. For this case, new charging stations are planned to load point 3, 15 and 31. Thereby, apply the proposed approach to the newly planned system, battery exhaustion locations can be found in Fig. 10(b). It can be seen that with the newly built charging stations, the total quantity of red points are remarkably reduced, indicating that fewer EVs have to face the battery depletion problem. Also, reliability indices of the planned system are presented in Table VIII. Comparing to Table II, it can be concluded that AFCH, ATCH and ATT indices are considerably decreased, while ATFC is slightly increased. This is because the probability for EVs to find a reachable charging station is enhanced in the planned system. In addition, the newly built charging stations have limited impact on the electrical power system.

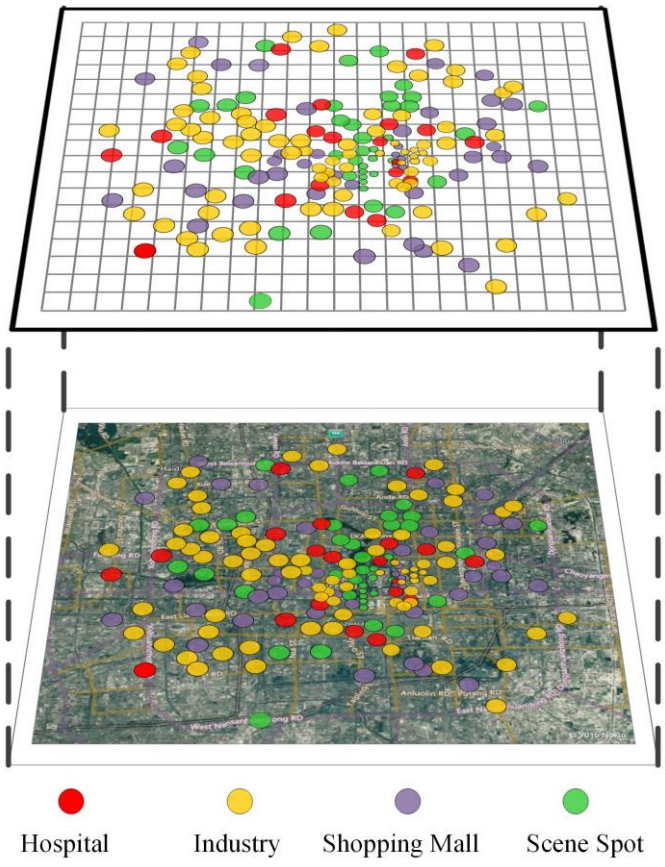

Fig. 11 Basic structure of the test system

B. A Large Scale Test System Case

In order to validate the practicality of the proposed approach, a large scale test system is created based on the transportation system of the central urban area of Beijing. Due to the lack of electrical system data of this city, we have to find a test case with similar scale to replace the original power grid. Notice that the peak load of this area is 2289 MW in 2013 [29], which is similar to the RTS system [25]. Then a test case is developed by combining the transportation system of Beijing central urban area and the RTS system, as shown in Fig. 11. Hospitals, industries, malls and scene spots are located by their practical locations in Beijing, and then assigned to their nearest buses in the RTS system. A perpendicular road system is also attached, whose distance between adjacent roads is set to 0.5 km. In additional, nine charging stations are introduced into this system.

Table IX Assessment results of the Beijing test case under various δ_{Ctl}

δ_{Ctl}	LOEE (MWh/y)	LOLP (times/y)	AFFC (times/y)	ATFC (h/y)	AFCH (times/y)	ATCH (h/y)	ATT (h/y)	EEG2V (MWh/y)	EEV2G (MWh/y)
100%	96950	0.0752	3.0827	3.2717	0.7409	1.3939	4.6655	0	0
80%	82866	0.0616	3.6151	3.7117	1.2932	2.6574	6.3691	34062	34753
60%	63233	0.0552	4.3401	4.6542	1.6254	3.4223	8.0765	65662	64944
40%	37809	0.0340	5.7268	6.2601	2.3892	5.2826	11.5427	59684	53317
20%	35551	0.0319	11.3930	12.3097	3.3484	6.8612	19.1709	61656	52119
0%	32525	0.0301	22.8054	29.9340	4.7113	9.3867	39.3207	63369	51676

They are scatteredly located so as to maximize the service area, as shown in Fig. 11. The total vehicle number of this area is one million, and EV penetration is assumed to be 10%. Other parameters are the same with the RBTS based system.

The proposed approach is applied to this system and test cases with various δ_{Ctl} are studied, as shown in Table IX.

It can be seen from the table that all quantitative reliability indices can be achieved. Comparing to the RBTS based test case, LOEE and LOLP are much larger in this case. However, differences of transportation indices are relatively small in this case. This is because both LOEE and LOLP are system level indices, which are relevant to system scale. Yet, transportation indices are average value for each EV in the system, and are almost irrelevant to the size of system.

It can be also noticed that, similar to the RBTS based test cases, with the decrease of δ_{Ctl}, power system reliability is enhanced, while transportation system reliability is slightly decreased. Therefore, case studies similar to Fig. 8 are performed to determine the optimal value of δ_{Ctl}, as shown in Fig. 12.

It can be seen that the LOEE curve is generally an ascending function of δ_{Ctl}, while the ATT curve is a descending one. However, when δ_{Ctl} drops below 40%, LOEE is considerably low, and ATT decreases dramatically. In general, when δ_{Ctl} =40%, both LOEE and ATT are acceptable. Therefore, the optimal value of δ_{Ctl} should be set to about 40%.

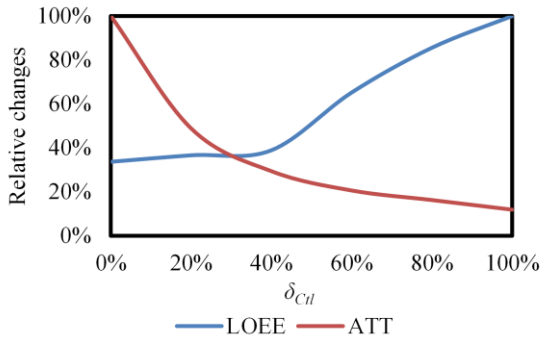

Fig. 12 Variation curve of LOEE and ATT

V. Conclusion

This paper studied the reliability assessment of integrated transportation and electrical power systems with considering the integration of renewable generations and electric vehicles. A bidirectional charging control strategy was first demonstrated to capture the interaction between the two systems. A simplified transportation simulation method was then developed, whose high efficiency made the reliability assessment of the ITES realizable with an acceptable accuracy. Also, a series of quantified reliability indices were defined for the integrated system. Thereafter, a daily periodic quasi sequential reliability assessment approach was developed for the ITES by combining the transportation simulation method to the generation adequacy evaluation algorithm. With the proposed approach, reliability indices of both power and transportation systems could be obtained. In addition, the impact of EV charging control techniques, involving both G2V and V2G controls, on the overall reliability of the two systems was analyzed in detail.

The results demonstrated the validity and practicality of the proposed approach. It could also prove that the implementation of EV charging controls would benefit the reliability of the power system, and was adverse to the transportation system. With the proposed method, the optimal EV charging control strategies could be obtained to balance the reliability of the two systems. Further analysis was also performed to investigate the impact of RG and EV penetration. It was also indicated that with EV charging control techniques, higher RG and EV penetration could be supported by a given power system without seriously affect the overall reliability. In addition, reliability based charging station planning could be performed with the proposed approach.

Reference

[1] J. Davies, "Using Dynamic Scenario Analyses to Evaluate How Market Factors Could Shape San Diego California New Car Buyer's Interest in Purchasing a Plug-in Electric Vehicle (PEV)", *Electric Vehicle Symposium and Exhibition (EVS27)*, Barcelona, pp. 1-10, 2013.

[2] T. Mai, M. M. Hand, S. F. Baldwin, et al, "Renewable Electricity Futures for the United States", *Sustainable Energy, IEEE Transactions on*, vol. 5, no. 2, pp. 372-378, 2014.

[3] C. Huang, F. Li, Z. Jin, "Maximum Power Point Tracking Strategy for Large-Scale Wind Generation Systems Considering Wind Turbine Dynamics," *Industrial Electronics, IEEE Transactions on* , vol. 62, no. 4, pp. 2530-2539, 2015.

[4] C. Huang, F. Li, T. Ding, Z. Jin, X. Ma, "Second-Order Cone Programming-Based Optimal Control Strategy for Wind Energy Conversion Systems Over Complete Operating Regions," *Sustainable Energy, IEEE Transactions on*, vol. 6, no. 1, pp. 263-271, 2015.

[5] P. Yang, A. Nehorai, "Joint Optimization of Hybrid Energy Storage and Generation Capacity with Renewable Energy", *Smart Grid, IEEE Transactions on*, vol. 5, no. 4, pp. 1566-1574, 2014.

[6] H. Cui; F. Li; X. Fang; R. Long, "Distribution network reconfiguration with aggregated electric vehicle charging strategy," *IEEE Power & Energy Society General Meeting*, Denver, pp.1-5, 2015.

[7] Z. Liu, D. Wang, H. Jia, et al, "Aggregation and Bidirectional Charging Power Control of Plug-In Hybrid Electric Vehicles: Generation System Adequacy Analysis", *Sustainable Energy, IEEE Transactions on*, In Press, pp. 1-11, 2014.

[8] Z. Liu, D. Wang, H. Jia, et al, "Power System Operation Risk Analysis Considering Charging Load Self-Management of Plug-In Hybrid Electric Vehicles", *Applied Energy*, vol. 136, pp. 662-670, 2014.

[9] S. Shao, M. Pipattanasomporn, S. Rahman, "Grid Integration of Electric Vehicles and Demand Response with Customer Choice", *Smart Grid, IEEE Transactions on*, vol. 3, no. 1, pp. 543-550, 2012.

[10] Y. Mu, J. Wu, N. Jenkins, et al, "A Spatial – Temporal Model for Grid Impact Analysis of Plug-In Electric Vehicles", *Applied Energy*, vol. 114, pp. 456-465, 2014.

[11] Q. Yu, N. Abi-Samra, "The Study of Demand for Electric Vehicles and Capability of Services Based on Behavior", *Doctor Thesis*, Shangdong University, 2014.

[12] S. Hu, C. Wang, "Vehicle Detector Deployment Strategies for the Estimation of Network Origin-Destination Demands Using Partial Link Traffic Counts", *Intelligent Transportation Systems, IEEE Transactions on*, vol. 9, no. 2, pp. 288-300, 2008.

[13] B. Falahati, Y. Fu, Z. Darabi, et al, "Reliability Assessment of Power Systems Considering the Large-Scale PHEV Integration", in *Vehicle*

Power and Propulsion Conference (VPPC), IEEE, Chicago, IL, pp. 1-6, 2011.
[14] R. C. Green, L. Wang, M. Alam, et al, "Evaluating the Impact of Plug-in Hybrid Electric Vehicles on Composite Power System Reliability", *North American Power Symposium (NAPS)*, Boston, MA, pp. 1-7, 2011.
[15] M. Fotuhi-Firuzabad, R. Billinton, "Impact of Load Management On Composite System Reliability Evaluation Short-Term Operating Benefits", *Power Systems, IEEE Transactions on*, vol. 15, no. 2, pp. 858-864, 2000.
[16] W. Liu, M. Zhang, B. Zeng, et al, "Analyzing the Impacts of Electric Vehicle Charging on Distribution System Reliability", in *Innovative Smart Grid Technologies - Asia (ISGT Asia)*, IEEE, pp. 1-6, 2012.
[17] L. Cheng, Y. Chang, J. Lin, et al, "Power System Reliability Assessment with Electric Vehicle Integration Using Battery Exchange Mode", *Sustainable Energy, IEEE Transactions on*, vol. 4, no. 4, pp. 1034-1042, 2013.
[18] D. Huang, R. Billinton, "Effects of Load Sector Demand Side Management Applications in Generating Capacity Adequacy Assessment", *Power Systems, IEEE Transactions on*, vol. 27, no. 1, pp. 335-343, 2012.
[19] J. L. Bowman, Ben-Akiva, "Activity-Based Disaggregate Travel Demand Model System with Activity Schedules", *Transportation Research Part A*, vol. 35, no. 1, pp. 1 - 28, 2001.
[20] Q. Yu, X. Han, "Distribution Efficiency Analysis of Battery Swapping Station Considering Road Cost", Automation of Electric Power Systems, vol. 38, no. 12, pp. 81-87, 2014.
[21] W. Li, "Risk Assessment of Power Systems Models, Methods, and Applications", John Wiley & Sons, 2014.
[22] K. Hou, H. Jia, X. Xu, Z. Liu and Y. Jiang, "A Continuous Time Markov Chain Based Sequential Analytical Approach for Composite Power System Reliability Assessment, " *Power Systems, IEEE Transactions on*, vol. 31, no. 1, pp. 738-748, 2016.
[23] A. M. Leite da Silva, R. A. González-Fernández, W. S. Sales, et al, "Reliability assessment of time-dependent systems via quasi-sequential Monte Carlo simulation" in *Probabilistic Methods Applied to Power Systems (PMAPS), 2010 IEEE 11th International Conference on*, IEEE, pp. 697-702, 2010.
[24] R. Billinton, J. Oteng-Adjei, S. Kumar, et al, "A Reliability Test System for Educational Purposes-Basic Data", *Power Systems, IEEE Transactions on*, vol. 4, no. 3, pp. 1238-1244, 1989.
[25] P. M.Subcommittee, "IEEE Reliability Test System", *Power Apparatus and Systems, IEEE Transactions on*, vol. PAS-98, no. 6, pp. 2047-2054, 1979.
[26] "Distributed Energy Resources Web Optimization Service (DER-CAM)", http://der.lbl.gov/der-cam, accessed 2015.
[27] R. N. Allan, R. Billinton, I. Sjarief, et al, "A Reliability Test System for Educational Purposes-Basic Distribution System Data and Results", *Power Systems, IEEE Transactions on*, wol. 6, no. 2, pp. 813-820, 1991.
[28] K. Qian, C. Zhou, M. Allan, et al, "Modeling of Load Demand Due to EV Battery Charging in Distribution Systems", *Power Systems, IEEE Transactions on*, vol. 26, no. 2, pp. 802-810, 2011.
[29] "Load demand of Beijing central area breaks the record for three times", http://www.cpnn.com.cn/dw/201308/t20130816_602414.html, accessed 2015.

APPENDIX

Before performing the time discretization technique, a continuous time Markov chain (CTMC) model should be create for the objective system. Define $X(t)$ as a random variable describing the impact of component outages at any given time t, then $\{X(t)\}$ is the created CTMC. The explicit process can be found in [21] or [22]. Its state space vector is $\boldsymbol{\Omega}_X=[x_1, x_2, \dots, x_n]$ and stationary distribution vector is $\boldsymbol{\pi}=[\pi_1, \pi_1, \dots, \pi_n]$. The state transition probability matrix $\boldsymbol{P}(t)$ can be obtained by the Kolmogorov forward equation

$$\mathbf{P}'(t)=\mathbf{Q}\mathbf{P}(t) \tag{A1}$$

Given the initial condition $p_{ij}(0)=\delta_{ij}$, the solution of (A1) is

$$\mathbf{P}(t)=\exp(t\mathbf{Q}) \tag{A2}$$

When the stationary distribution is reached, the mean function $m(t)$ and auto-covariance function $\Gamma(t+\tau,t)$ are

$$m(t)=E\left[X(t)\right]=\pi\,\Omega^{\mathrm{T}} \tag{A3}$$

$$\begin{aligned}\Gamma(t+\tau,t)&=E\left[X(t+\tau)X(t)\right]\\&=\sum_{i=1}^{n}\sum_{j=1}^{n}x_j x_i p_{ij}(\tau)\pi_i=\boldsymbol{\Omega}_{\pi}\cdot\mathbf{P}(\tau)\cdot\boldsymbol{\Omega}^{\mathrm{T}}\end{aligned} \tag{A4}$$

where $\boldsymbol{\Omega}_{\pi}=[x_1\pi_1, x_2\pi_2, \dots, x_n\pi_n]$.

As shown in (A3) and (A4), $m(t)$ is constant and $\Gamma(t+\tau, t)$ is independent from t. Thus, $\{X(t)\}$ is a stationary process. Then the power spectral function $F(\lambda)$ and density function $f(\lambda)$ are

$$f(\lambda)=2\int_0^{+\infty}\cos t\lambda\,\Gamma(t)\,dt \tag{A5}$$

$$F(\lambda)=\int_{-\infty}^{\lambda}f(\lambda)\,d\lambda \tag{A6}$$

The sampling theorem of stationary process is presented as

$$\int_{|\lambda|\geq 2\pi\alpha}f(\lambda)d\lambda=0 \tag{A7}$$

where α is the upper bound frequency.

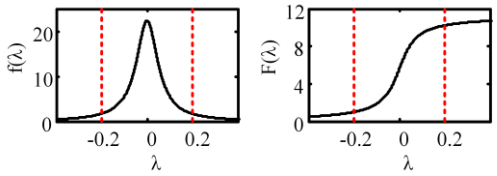

Fig. A1. The power spectral function and its density function.

If (A7) is satisfied, then $\{X(t)\}$ contains no frequencies higher than α and the sampling interval is $\Delta t=(2\alpha)^{-1}$. However, $\{X(t)\}$ is not band limited for power systems, as shown in Fig. A1. So there is no upper bound frequency theoretically. Thus, a threshold δ_{PS} is set to estimate a reasonable α. According to the properties of power spectral function, we know

$$F(+\infty)=\int_{-\infty}^{+\infty}f(\lambda)\,d\lambda=2\pi\Gamma(0) \tag{A8}$$

where $F(+\infty)$ is the total power of $\{X(t)\}$.

The threshold δ_{PS} can be set as a promotion of the total power $F(+\infty)$. By ignoring the high frequency part, which contains power no more than δ_{PS}, α can be obtained by

$$\int_{|\lambda|\geq 2\pi\alpha}f(\lambda)\,d\lambda=\delta_{\mathrm{PS}}F(+\infty) \tag{A9}$$

After α is obtained, the sampling interval is decided by $\Delta t=(2\alpha)^{-1}$ and the sampling frequency is $N_{\mathrm{SF}}=\Delta t^{-1}$. Before further analysis, we can amplify N_{SF} to an integer and modify Δt accordingly. Then the sample sequence of the newly created discrete time Markov chain model is $\{X(k\Delta t), k=0,1,\dots, N_{\mathrm{SF}}\}$. $\boldsymbol{p}_{k\Delta t}$ represents the probability distribution of impact states at time $k\Delta t$, which is decided by

$$\mathbf{p}_{k\Delta t}=\mathbf{p}_{(k-1)\Delta t}\mathbf{P}(\Delta t) \tag{A10}$$

It is necessary to consider the fluctuation of the load level. From (A4) we know that the $\Gamma(t)$ is related to the value of x_i. When load level drops, x_i also decreases, causing decline of $\Gamma(t)$, $F(\lambda)$, $F(+\infty)$ and the obtained N_{SF}. To be conservation, the maximum load level is used to calculate N_{SF}.

Kai Hou (S'15) received his B.S. and M.S. degrees in the electrical engineering and automation from Tianjin University, Tianjin, China.

He is currently pursuing the Ph.D. degree in the Electrical Engineering Department, Tianjin University. His research interests include reliability and risk assessments of power system, integrated energy system, and smart grid.

Xiandong Xu (M'15) received his Ph.D. degree in electrical engineering in 2015 from Tianjin University, Tianjin, China.

Currently, he is working as a research fellow at Queen's University Belfast, UK. His research focuses on energy infrastructure modeling, energy management, and reliability analysis.

Hongjie Jia (M'04) received his Ph.D. degree in electrical engineering in 2001 from Tianjin University, China.

He became an Associate Professor at Tianjin University in 2002, and was promoted as Professor in 2006. His research interests include power reliability assessment, stability analysis and control, distribution network planning and automation, and smart grids.

Xiandan Yu received his B.S., M.S. and Ph.D degrees in the electrical engineering from Tianjin University, Tianjin, China.

She is currently an associate professor in at Tianjin University. Her research interests include power system stability, integrated energy system, electric circuit theory and smart grids.

Tao Jiang (M'15) received the B.S. and M.S. degrees in electrical engineering from Northeast Dianli University, Jilin, China, in 2006 and 2011, respectively, and the Ph.D. degree in electrical engineering from Tianjin University, Tianjin, China, in 2015.

He is presently an Associate Professor with the Department of Electrical Engineering, Northeast Dianli University, Jilin, JL, China. He was with the Department of Electrical and Computer Engineering, North Carolina State University, Raleigh, NC, USA, as a visiting scholar from 2014 to 2015. His research interests include power system stability analysis and control, renewable energy integration, demand response, and smart grid.